Ordine degli Ingegneri della Provincia di Roma

AGI G

AGI Associazione Geotecnica Italiana

5° IAGIG

Incontro Annuale dei Giovani Ingegneri Geotecnici

22 e 23 Maggio 2015

Aula Magna, Università Europea,
Via degli Aldobrandeschi, 190 Roma

Patrocinato da:

CONSIGLIO NAZIONALE DEGLI INGEGNERI

Società Italiana Gallerie
Italian Tunnelling Society

Consiglio Nazionale delle Ricerche

Istituto Nazionale di Geofisica e Vulcanologia

oice
Associazione delle organizzazioni di ingegneria di architettura e di consulenza tecnico-economica
CONFINDUSTRIA

fastigi
FORMAZIONE ADDESTRAMENTO SCIENZA TECNOLOGIA INGEGNERIA GALLERIE E INFRASTRUTTURE

Liquefaction analysis with the use of The finite element code PLAXIS

Anita Laera (al@plaxis.com)
Plaxis bv
Ronald B.J. Brinkgreve (rbj@plaxis.com)
Geo-Engineering section, Delft University of Technology, Delft, The Netherlands

ABSTRACT. In this paper a liquefaction analysis is performed using two different approaches: the semi-empirical procedure from Idriss and Boulanger, and a site response analysis performed with the finite element code PLAXIS 2D, using a constitutive model that accounts for pore pressure accumulation in saturated cohesionless soils under cyclic loading. The results show a good comparison between the numerical model and the conventional approach.

1. Introduction

When an earthquake occurs, the seismic waves propagate from the source till the ground surface, causing ground shaking. The effects of an earthquake can be different, such as structural damages, landslides and soil liquefaction. To establish if liquefaction is likely to occur in a specific site subjected to a selected earthquake, semi-empirical procedures or dynamic methods can be used. The semi-empirical procedures consist in the evaluation of a safety factor as the ratio of the cyclic shear stress required to cause liquefaction and the equivalent cyclic shear stress induced by the earthquake. The dynamic methods are based on site response analysis in terms of total or effective stresses.
In this paper a comparison between the simplified procedure from Idriss and Boulanger (2014) and a site response analysis performed with the use of the finite element code PLAXIS 2D is presented.

2. Case description

The in situ characterization leads to the following soil stratigraphy: a clay layer extends from the ground surface to 5 m depth and is followed by 10 m of loose or medium loose sand for which 5 SPT measurements are performed every 2 meters (Table 1). The in situ tests are performed till a depth of 40 m, where a rock-like formation has been identified. The material from 15 to 40 m is characterized by moderate stiff clay. The shear wave velocity varies with depth as in Figure 1a, with a minimum v_s of 113 m/s at the top of the clay layer. The water table is coincident with the ground surface level. The ground surface, the layers and the bedrock surface are horizontal and extend to infinity. A one-dimensional wave propagation can be performed. The target acceleration-time history is a modified Loma Prieta recording, scaled to a peak ground acceleration of 0.3 g, recorded at the outcrop of a rock formation and characterized by a magnitude Mw of 6.9 and a duration of 40 seconds (Figure 1b).

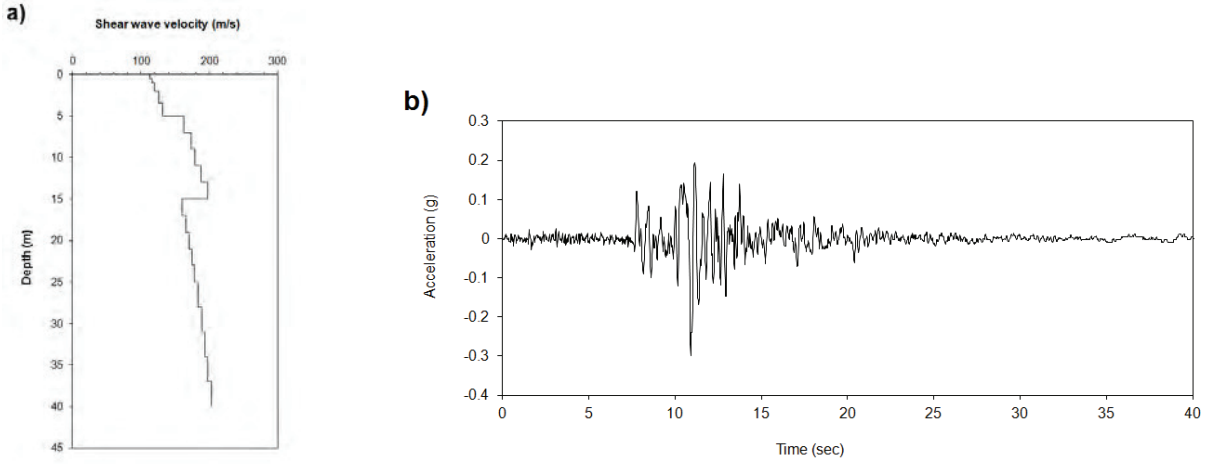

Figure 1. Shear wave velocity profile (a),input earthquake scaled at the maximum acceleration of 0.3 g (b).

3. Simplified procedure for triggering liquefaction

The semi-empirical procedure to evaluate liquefaction potential during earthquakes consists in the evaluation of a safety factor given by the ratio of the cyclic resistance ratio CRR, i.e. the capacity of the soil to resist liquefaction (determined on case histories), and the cyclic stress ratio CSR, i.e. the equivalent cyclic shear stress induced by the earthquake (Seed and Idriss, 1971). According to Eurocode 8, liquefaction can occur when the safety factor is less than 1.25.
For all the 5 sand layers, the following normalized penetration resistance are calculated and the liquefaction resistance of each layer can be determined from the chart (Table 1). As concluded from this simplified analysis, all sand layers are likely to liquefy under the given earthquake condition.

Depth	Nspt	$(N_1)_{60}$	CSR $_{M=7.5 \mid \sigma v = 1 atm}$	CRR	FS
5	5	8.09	0.435	0.11	0.24
7	7	9.97	0.444	0.12	0.27
9	6	7.72	0.446	0.10	0.23
11	8	9.46	0.440	0.11	0.26
13	10	11.00	0.431	0.13	0.29

Table 1. SPT blow counts, normalized penetration resistance, normalized CSR ratio, liquefaction resistance and safety factor.

4. Definition of the numerical model in PLAXIS

A one-dimensional wave propagation can be performed. In PLAXIS 2D, a soil column is modeled where the horizontal dimension is chosen equal to 2.5 m, according to the required element length (Kuhlemeyer and Lysmer, 1973). Eight soil layers are specified considering a clay layer above and below the sand deposit, that is discretized into 5 layers according to the available N_{SPT} measurements. The bottom layer is modeled as a rock formation.

In general, when the soil is subjected to cyclic shear loading, it shows a non linear and dissipative behaviour, i.e. the soil stiffness varies with depth and its value decays with the strain level induced by the loading. To account for these aspects, the Generalized Hardening Soil material model, based on the HSsmall model, is used. In this example, some of the characteristics of the HSsmall material model are kept, such as the strain dependent stiffness and the stress dependency formula, i.e.:

$$G_0 = G_0^{ref}\left(\frac{c\cdot\cos\varphi - \sigma'_3\cdot\sin\varphi}{c\cdot\cos\varphi + p^{ref}\cdot\sin\varphi}\right)^m \quad (1)$$

Differently from the HSsmall, the GHS model allows to consider the stiffness dependent on the stress level at the beginning of the calculation phase and to activate only the Mohr-Coulomb failure criterion to avoid the overdamping caused by the generated plastic strains.

The parameters of the model are calibrated according to some considerations since no data are available. The shear strain $\gamma_{0.7}$ is taken equal to 0.0007 and has been calibrated to get the best fit between both the calculated G_s/G_0 and the theoretical curve that expresses the decay of the shear modulus with strain (Figure 2) and the calculated damping curve and the one representative of the considered type of soil (Figure 3). The reference G_s/G_0 curve (Figure 2) is described in literature by Vucetic and Dorby (1991) for a plasticity index PI of 50% (in blue). The shear strain that corresponds to the point in which the secant shear stiffness G_t reaches the limit value of G_{ur} represents the cut-off shear strain $\gamma_{cut\text{-}off}$, i.e. the limit above which the shear stiffness cannot decrease more than the reached G_{ur}. The damping ratio evolves as a function of the shear strain and it increases for larger values of γ. Figure 5 represents the best fitting reached in this case, compared to the curve determined by Vucetic and Dobry (1991) for a clay characterized by PI equal to 50%.

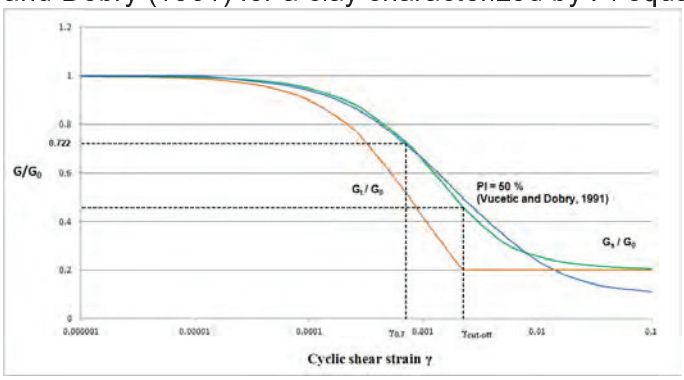

Figure 2. Shear modulus reduction curves.

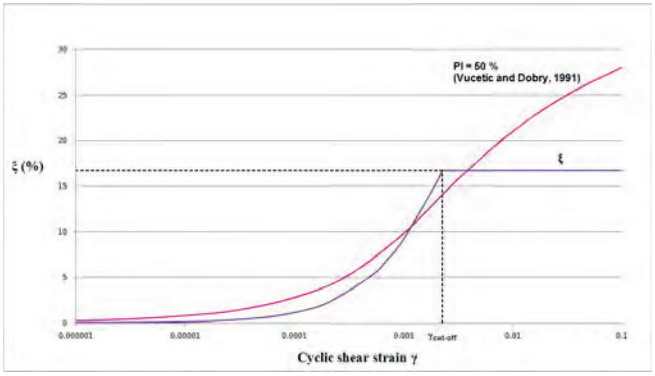

Figure 3. Damping curves.

The initial shear stiffness at the reference pressure, G_0^{ref}, is taken equal to 48000 kN/m^2 in order to have a good approximation of the shear modulus variation with depth in the clay layer, considering that the cohesion is 10 kN/m^2, the friction angle is 26° and m is 0.6. Setting the ratio G_0^{ref} over G_{ur}^{ref} equal to 5, the corresponding G_{ur}^{ref} is taken equal to 9600 kN/m^2. For υ_{ur} equal to 0.2, E_{ur}^{ref} is 23040 kN/m^2, while E_{50}^{ref} and E_{oed}^{ref} are taken as 1/3 of E_{ur}^{ref}, i.e. 7680 kN/m^2.

As for the drainage type, considering that the soil is totally saturated and earthquakes act for a very short time, the Undrained A option has been chosen, which implies that PLAXIS will automatically add a large bulk modulus for the pore water.

For the undrained dynamic calculation the UBC3D-PLM model is used in order to properly model the evolution of the excess pore pressures in the sandy soils and capture the onset of liquefaction. The complete description of the model can be found in literature (Petalas and Galavi, 2013). The model parameters are based on N_{SPT} values. Beaty and Byrne (2011) proposed a set of equations based on $(N_1)_{60}$ for the initial generic calibration of the UBCSAND 904aR model. Makra (2013) revised the proposed equations and highlighted the differences between the UBCSAND 2D formulation and the UBC3D-PLM model, as implemented in PLAXIS.

All the 5 sand layers are modeled with UBC3D-PLM with Undrained A condition and with γ_{unsat} and γ_{sat} equal to 14 and 18 kN/m^3, respectively. The set of parameters used for this example can be found in Table 2, where φ_p is the peak friction angle, φ_{cv} is the friction angle at constant volume, K_G^e is the elastic shear modulus, K_G^p is the plastic shear modulus and K_B^e is the elastic bulk modulus. R_f is the faliure ratio. The friction angle φ_{cv} has been determined for each layer considering a correlation between the N_{SPT} number and the vertical effective stress. As for the power for stress dependency of the bulk and shear moduli, m^e, n^e and n^p, the default values of 0.5, 0.5 and 0.4 respectively, are used. It is suggested to choose a densification factor fac_{hard} of 1.0 and a coefficient of 1.0 for the fac_{post}.

Parameter	Sand layer 1	Sand layer 2	Sand layer 3	Sand layer 4	Sand layer 5	Unit
φ_{cv}	29.2	33	29.2	32.1	32.9	Degrees
φ_p	30	34	30	33	34	Degrees
K_G^e	870.65	933.3	857	917	964	-
K_G^p	271	378	253	346	450	-
K_B^e	609.5	653	600	642	675	-
R_f	0.804	0.779	0.810	0.785	0.768	-
$(N_1)_{60}$	8.09	9.97	7.72	9.46	11	-

Table 2. Material parameters for the sand layers (UBC3D-PLM model).

To generate the initial stress state correctly, it is necessary to perform the initial phase using the Hardening Soil model with parameters calibrated for the same sand. Hysteretic damping of the soil model can capture damping at strains larger than 10^{-4} – 10^{-2} %, but to account for the irreversible behaviour of the soil at lower deformation levels, Rayleigh damping coefficients, α and β, equal to 0.09635 and 0.0007899, respectively, and corresponding to a target damping ratio of 1% are used. The rock formation at the basis of the model has been modeled through a linear elastic material model with drained condition and a high shear wave velocity (about 1220 m/s) (γ= 22 kN/m^3, E = 8.011E6, u=0.2).

The earthquake is input as a prescribed displacement at the bottom boundary, modelled as a compliant base. An interface is defined at the bottom to create a so called node pair: it is possible to both apply the input motion and absorb the incoming waves (Galavi et al. 2013). PLAXIS transfers the input motion to the main domain by applying equivalent forces, which are internally calculated considering the mechanical properties of the layer at the base of the model and the upward motion. Since the earthquake is recorded at the outcrop of a rock formation, it consists of the superposition of the upward and downward propagating waves with same amplitudes. In this case the input signal is taken as half of the outcropping motion.

For the lateral boundaries, tied degrees of freedom are used, since they allow to model a reduced geometry of the problem: the nodes at the left and right model boundaries are connected to each other and are characterized by the same displacement.

5. Results

The liquefaction potential can be expressed by means of the excess pore pressure ratio r_u, which represents the ratio of the excess pore pressure and the initial effective vertical stress at that depth.

For the UBC3D-PLM model, r_u is given by:

$$r_u = 1 - \frac{\sigma'_v}{\sigma'_{v0}} \tag{2}$$

where σ'_v is the vertical effective stress at the end of the dynamic calculation and σ'_{v0} is the initial effective vertical stress prior to the seismic motion. Beaty and Perlea (2011) consider zones with a maximum r_u greater than 0.7 to be liquefied. Figure 4a shows that liquefaction occurs in all the five sand layers, since the r_u parameter is about 1 at the end of the analysis. The values of the excess pore pressures in those layers are very high (Figure 4b) and consequently, the effective stresses are almost zero (Figure 4c). The results from the PLAXIS liquefaction analysis are in good agreement with the results of the simplified liquefaction analysis.

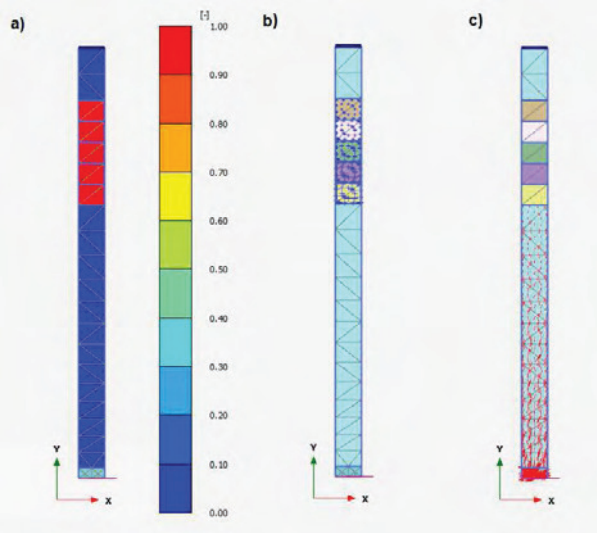

Figure 4. Pore pressure ratio r_u at the end of the analysis (a), excess pore pressure (b) and principal effective stress (c).

6. Conclusion

This paper presents the results of a dynamic analysis performed with the PLAXIS finite element code, aimed at modelling the onset of liquefaction in loose cohesionless soils. Two different approaches, commonly used in engineering practice, are compared. First, the simplified procedure introduced by Seed and Idriss (1971) and updated by Idriss and Boulanger (2014) is carried out. The onset of liquefaction is determined by a curve which separates a liquefiable state from a non liquefiable state. This curve is built on the basis of a large number of case-histories. The second approach consists of a fully dynamic analysis by means of the finite element code Plaxis 2D. In this case, the dynamic boundary conditions and the selection of appropriate consitutive models to reproduce the behaviour of saturated soils under cyclic loads are essential.

The comparison between the two approaches can be considered satisfactory, since the onset of liquefaction is successfully modeled in all the five sand layers. The UBC3D-PLM model can be considered capable of modelling the accumulation of the excess pore pressures in saturated cohesionless soils and can be used to predict the cyclic behaviour of sands with high accuracy.

7. Bibliography

Beaty M.H, Perlea V.G. (2011). Several observations on advanced analyses with liquefiable materials. *Thirty first annual USSD conference on 21st century dam design-advances and adaptations. San Diego, California, 11-15 April 2011. US society on dams, Denver*, 1369-1397.

Galavi V., Petalas A., Brinkgreve R.B.J. (2013). Finite element modeling of seismic liquefaction in soils. *Geotechnical Engineering Journal of Ihe SEAGS &AGSSEA.* 44 (3): 55-64.

Idriss I. M., Boulanger R.W. (2014). CPT and SPT based liquefaction triggering procedures. *Report UCD/CGM-14/01, Department of Civil and Environmental Engineering, University of California, Davis, CA*.

Kuhlemeyer R.L., Lysmer J. (1973). Finite element method accuracy for wave propagation problems. *Journal of the Soil Mechanics and Foundations Division*, 99 (5): 421-427.

Makra A. (2013). Evaluation of the UBC3D-PLM constitutive model for prediction of earthquake induced liquefaction on embankment dams. *MSc Thesis, TU Delft*.

Petalas A., Galavi V. (2013). Plaxis liquefaction model UBC3d-PLM. *Plaxis knowledge base.* www.plaxis.com.

Seed H.B, Idriss I.M. (1967). Analysis of liquefaction: Niigata earthquake. *Proc. ASCE*, 93 (SM3): 83-108.

Seed H.B, Idriss I.M. (1971). Simplified procedure for evaluating soil liquefaction potential. *Journal of the Soil Mechanics and Foundations Division*, 97 (9): 1249-1273.

Vucetic M., Dobry R. (1991). Effect of soil plasticity on cyclic response. *Journal of Geotechnical Engineering, ASCE,* 117 (GT1): 89-107.